Article

The Ionic Organic Cage: An Effective and Recyclable Testbed for Catalytic CO$_2$ Transformation

Wenlong Wang [1,*], Yuanyou Mao [1,2], Jutao Jin [1], Yanping Huo [2,*] and Lifeng Cui [1,*]

1   School of Materials Science and Engineering, Dongguan University of Technology, Dongguan 523808, China; maoyuanyou126@126.com (Y.M.); jinjt@dgut.edu.cn (J.J.)
2   School of Chemical Engineering and Light Industry, Guangdong University of Technology, Guangzhou 510006, China
*   Correspondence: wangwl@dgut.edu.cn (W.W.); yphuo@gdut.edu.cn (Y.H.); lcui@dgut.edu.cn (L.C.)

Abstract: Porous organic cages (**POC**) are a class of relatively new molecular porous materials, whose concept was raised in 2009 by Cooper's group and has rarely been directly used in the area of organic catalysis. In this contribution, a novel ionic quasi-porous organic cage (denoted as **Iq-POC**), a quaternary phosphonium salt, was easily synthesized through dynamic covalent chemistry and a subsequent nucleophilic addition reaction. **Iq-POC** was applied as an effective nucleophilic catalyst for the cycloaddition reaction of CO$_2$ and epoxides. Owing to the combined effect of the relatively large molecular weight (compared with PPh$_3$$^+I^-$) and the strong polarity of **Iq-POC**, the molecular catalyst **Iq-POC** displayed favorable heterogeneous nature (i.e., insolubility) in this catalytic system. Therefore, the **Iq-POC** catalyst could be easily separated and recycled by simple centrifugation method, and the catalyst could be reused five times without obvious loss of activity. The molecular weight augmentation route in this study (from PPh$_3$$^+I^-$ to **Iq-POC**) provided us a "cage strategy" of designing separable and recyclable molecular catalysts.

Keywords: organic cage; carbon dioxide; catalyst recycling; triphenylphosphine; quaternary phosphonium salt
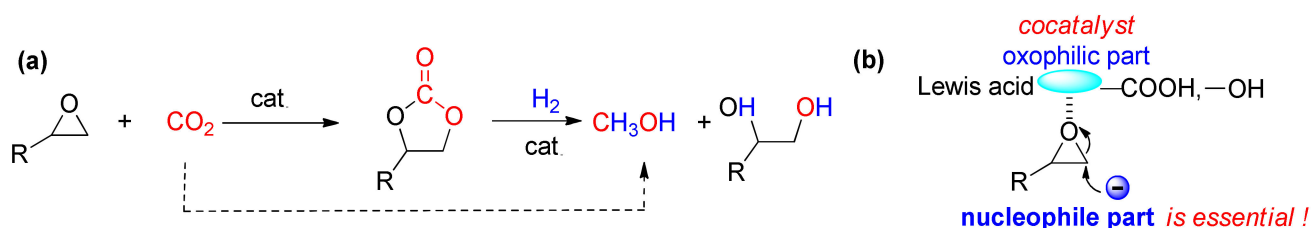
1. Introduction

In 2009, Cooper and co-workers discovered a new type of 3D discrete molecular cages with a central cavity and molecule accessible windows, and then named them porous organic cages (**POC**) [1]. Research in this field has been on the rise in the last decade [2–11], with imine condensation [12–18] and boronic esters formation [19–26] being the two main strategies for constructing **POC** materials. When thinking at a higher level about the assembly, scientists found that **POC** materials are assembled by two organic synthons through dynamic covalent chemistry (DCC) [5], which means **POC** materials are constructed by reversible covalent bonds only, and this is the main characteristic that distinguishes them from other cage materials (such as metal-based coordination cages [27]). Due to their porous nature and "solution processable" feature, **POC** materials have found widespread application in the areas of gas storage and separation materials [28–33], host-guest chemistry [34–37], sensors [21,22,38–40], packing materials for chromatography [41–44] and synthetic templates for metal nanoparticles (MNPs) [45–54].

Despite the research of **POC** materials growing substantially in the last decade (**POC**-stabilized MNPs in catalysis are relatively common [47–59]), the direct using of pure **POC** molecules in catalysis has rarely been reported. To the best of our knowledge, only a few studies (less than five) have been reported. For instance, Smith and co-workers developed an iron porphyrin-decorated **POC** molecule as a highly efficient catalyst for electrochemical CO$_2$ reduction [60]. Jiang's group elaborated a tubular organic porphyrin cage and elucidated its heterogeneous photocatalytic superiority in the heterogeneous photo-oxidation of primary amines [61]. Very recently, Kim's group reported a gigantic porphyrin cage (**P$_{12}$L$_{24}$**,

built with 12 square-shaped porphyrins (**P**) and 24 bent linkers (**L**)), and it was applied as an efficient catalyst for the photooxidation of 1,5-dihydroxynaphthalene in the presence of oxygen and visible light [62]. Patra et al. reported an organic cage for catalytic CO_2 conversion [63]. In this contribution, we introduce a quaternary phosphonium salt-functionalized cage as an effective and recyclable catalyst for catalytic CO_2 transformation.

Today in the 21st century, the greenhouse gas CO_2, which is mostly produced by the burning of petroleum, coal and natural gas, is a big problem due to climate change, ocean acidification and the global sea-level rise [64]. On the other hand, CO_2 could be an economical, renewable, nontoxic and abundant source of carbon, and therefore an attractive C1 synthetic building block for some useful fine chemicals. Additionally, to a certain extent, the conversion of CO_2 into value-added fine chemicals helps the carbon cycle of the earth, which is a fascinating goal in the area of green chemistry and catalysis [65,66]. Notably, the transformation of CO_2 into cyclic carbonates has attracted much attention because of the extensive applications of cyclic carbonates, such as the electrolytes of lithium-ion batteries, polar aprotic solvents and important intermediates for fine chemicals [67–70]. Recent research suggested that cyclic carbonates can be straightforwardly converted to methanol (CH_3OH) and diols through a catalytic hydrogenation process, and this process might be an alternative pathway to produce CH_3OH from CO_2 (Scheme 1a) [71,72].

Scheme 1. (**a**) Transformation of CO_2 to cyclic carbonates and the subsequent hydrogenation reaction, and (**b**) the accepted activation mechanism of epoxide.

To synthesize the cyclic carbonates from epoxides and CO_2, a catalyst is essential during the ring-opening of epoxides. Various molecular catalysts have been developed to realize the ring-opening process of epoxides. However, in the end, in almost all cases, a nucleophile as the catalyst is essential for the reaction, and a cocatalyst (such as a Lewis acid and another oxophilic compound) is not essential, although the cocatalyst also plays an important role (Scheme 1b) [73]. Among the various nucleophiles reported, ionic liquids [74–76], quaternary ammonium salts [77–79] and quaternary phosphonium salts [80] are the three most recognized catalysts because of the powerful nucleophilicity of their counter anions. However, almost all the homogeneous nucleophile catalysts are hard to recover and reuse; therefore, from the viewpoint of green catalysis, it is necessary to develop a recyclable nucleophile catalyst [81]. In this contribution, a novel quasi-ionic porous organic cage (**Iq-POC**), a quaternary phosphonium salt, was synthesized and utilized as a recyclable nucleophile catalyst (Figure 1a). We came up with the name quasi-porous organic cages (**q-POC**) because their pore windows are too small for external molecules to enter their inner cavities (the crystal data and nitrogen adsorption experiment can prove that). From one point of view, our nucleophile cage catalyst **Iq-POC** could be viewed as an amplified version of methyltriphenylphosphonium iodide (**5**). As a matter of experience, small organic molecules with molecular weights (Mw) < 500 are generally soluble in common solvents; however, strongly polar compounds with large molecular weights (Mw) > 1000 are usually poorly soluble in common solvents. Therefore, the molecular amplifying process from methyltriphenylphosphonium iodide to **Iq-POC** can be understood as the heterogenized (from homogeneous to heterogeneous) process of a homogeneous catalyst. The synthetic route of the nucleophile catalyst **Iq-POC** is illustrated in Figure 1a. Two equivalents of triphenylphosphine-based tri-aldehyde (**1**) and three equivalents of (R,R)-1,2-cyclohexanediamine were assembled together ([2+3] assembly)

to afford the PPh$_3$-based cage compound (**3**) through dynamic covalent synthesis. The crystal structure of cage **3** is illustrated in Figure 1b, which provides us a clear idea of its structure by using different viewing angles. Subsequently, cage compound **3** was reacted with iodomethane—a nucleophilic reaction—to form the target molecule **Iq-POC** (Figure 1a; for detailed synthetic procedures and characterizations, see Supplementary Materials). The cage compound **Iq-POC** could be recognized as an amplified version of methyltriphenylphosphonium iodide (**5**), and **Iq-POC** exhibited very poor solubility in epoxides and cyclic carbonates; therefore, it could be easily separated and reused in the catalytic synthesis of cyclic carbonates through the solvent-free cycloaddition reaction of CO$_2$ and epoxides.
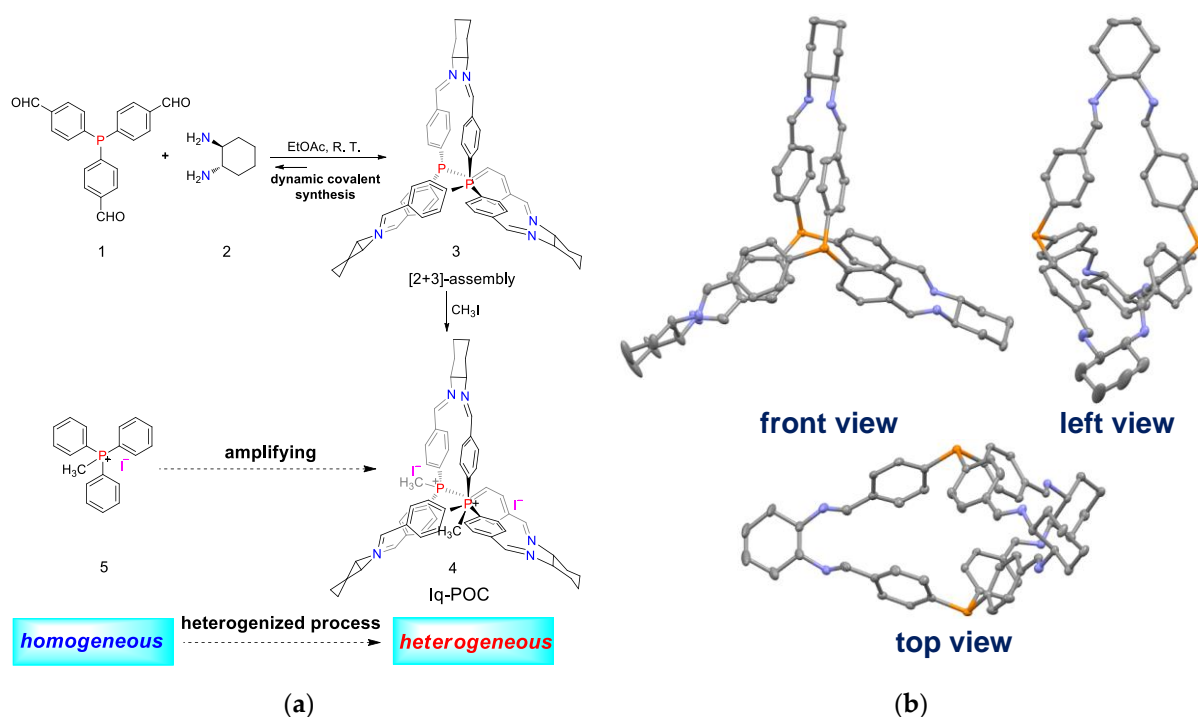

Figure 1. (**a**) Synthesis of the nucleophile catalyst ionic quasi-porous organic cage (**Iq-POC**), and (**b**) the crystal structure of cage **3** (H atoms are omitted for clarity; ellipsoids are drawn at 30% probability level). CCDC number: 1857683.

2. Results and Discussion

The synthesis of **Iq-POC** was mainly divided into two steps, i.e., the synthesis of cage **3** through dynamic covalent chemistry (DCC) and the subsequent nucleophilic addition reaction. DCC is essentially a kind of reversible chemistry which has a self-correcting function [5]. A subsequent nucleophilic addition reaction is frequently used in organic syntheses, and the yield (91%) in this case was high. The cage **Iq-POC** was poorly soluble in almost all solvents, so it could not be characterized by liquid nuclear magnetic resonance (NMR). However, we obtained the high-resolution mass spectra (HRMS) spectrum; its molecular weight can be measured at very dilute concentrations. The peak at $m/z = 478.2386$ corresponds to $[M - 2I]^{2+}$ (Figure 2, theoretical value: $m/z = 478.7412$, $z = 2$). To further confirm its structure, the solid-state ^{31}P NMR spectrum was obtained for our ionic cage, and the result showed just one signal at 22.0 ppm (see Supplementary Materials), which is the characteristic peak of a "quaternary phosphonium salt." The ^{31}P NMR peak of the cage **3** was at −7.8 ppm (very similar to PPh$_3$), which is quite different from that of a quaternary phosphonium salt. Moreover, the powder X-ray diffraction (PXRD) indicated the ionic cage was relatively amorphous (see Supplementary Materials), and the N$_2$ adsorption isotherm revealed the cage was nonporous (very low adsorbed volume; see Supplementary Materials), which could be ascribed to the narrow windows and dense

packing structure. With the prepared nucleophilic cage **Iq-POC** in hand, we then test the catalytic activities of **Iq-POC**/ZnX$_2$ catalysts toward cycloaddition of CO$_2$ and propylene oxide. For the sake of simplicity and cost, ZnX$_2$ combinations were chosen as the Lewis acid cocatalysts. The catalyst combination of **Iq-POC**/ZnBr$_2$ displayed better activity (turnover frequency (TOF) = 1550 h^{-1}, Table 1, entry 1) than **Iq-POC**/ZnCl$_2$ (TOF = 1050 h^{-1}, Table 1, entry 2) and **Iq-POC**/ZnI$_2$ (TOF = 1400 h^{-1}, Table 1, entry 3). The order of the activity of different Lewis acidic cocatalysts was found to be ZnBr$_2$ > ZnI$_2$ > ZnCl$_2$, which is constant with a previous report [73]. To check if the imine bonds of the cage play a role in the catalytic cycle, methyltriphenylphosphonium iodide (CH$_3$P$^+$Ph$_3$I$^-$)/ZnBr$_2$ was used as the catalyst; the iodide ion was taken as the active center; the CH$_3$P$^+$Ph$_3$I$^-$/ZnBr$_2$ system (Table 1, entry 6) exhibited slightly higher activity than the **Iq-POC**/ZnBr$_2$ system. This might be explained by the better solubility of CH$_3$P$^+$Ph$_3$I$^-$ compared with the amplified cage analogue; the result also told us the imine bonds have little effect on the catalytic cycle. When the Lewis acid cocatalyst ZnBr$_2$ was used alone, only a trace amount of propylene carbonate was afforded (Table 1, entry 4), which indicates that the nucleophilic cage **Iq-POC** is essential for the catalytic system. When the nucleophilic cage **Iq-POC** was used alone without the cocatalyst, only 2% yield of propylene carbonate was obtained (Table 1, entry 5), which implies the Lewis acidic cocatalyst also plays an important role in this case. With the optimized catalytic system of **Iq-POC**/ZnBr$_2$ in hand, we then investigated the effect of reaction time on the yield of propylene carbonate. As illustrated in Figure 3a, the conversion of propene epoxide proceeded relatively quickly within the first 1 h (31% yield of propylene carbonate was afforded). After 7 h, a yield of 87% was obtained, and then the yield reached a plateau; a high yield (>95%) could be obtained when the reaction time was longer than 9 h.
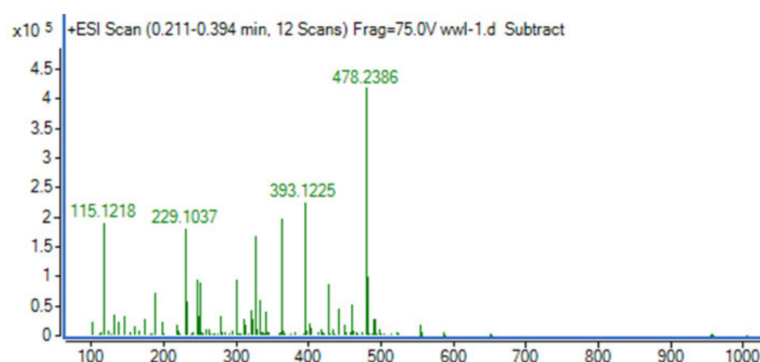

Figure 2. Electrospray ionization high resolution mass spectrometry (ESI-HRMS) of the cage **Iq-POC**.

Table 1. Catalytic activities of different catalytic systems in the cycloaddition reaction of CO$_2$ and propylene oxide [1].

Entry	Catalyst	Gas Chromatography (GC) Yield (%)	TOF (h^{-1})
1	**Iq-POC**/ZnBr$_2$	31	1550
2	**Iq-POC**/ZnCl$_2$	21	1050
3	Iq-POC/ZnI$_2$	28	1400
4	ZnBr$_2$	trace	—
5	Iq-POC	2	100
6	CH$_3$P$^+$Ph$_3$I$^-$/ZnBr$_2$	38	1900

[1] Reaction conditions: propylene oxide (2.9 g, 50 mmol), an initial pressure of 3 MPa CO$_2$, substrate/catalyst = 5000, **Iq-POC** (12.1 mg, 0.01 mmol), ZnX$_2$ (0.1 mmol), CH$_3$P$^+$Ph$_3$I$^-$ (8.1 mg, 0.02 mmol), 1 h, 120 °C. The selectivities of all the results were >99%. All the results were averaged over two runs.
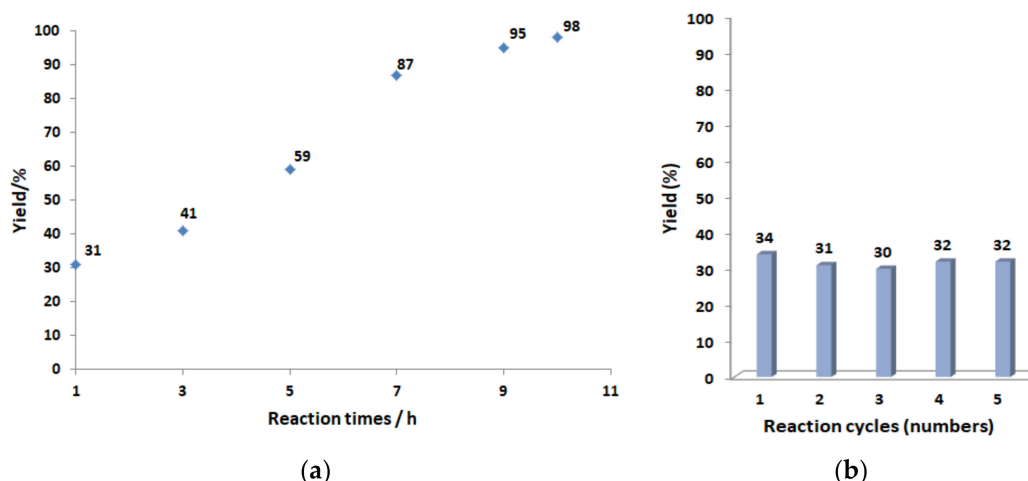
(a)

(b)

Figure 3. (**a**) Plot of GC yield versus reaction time. Reaction conditions: propylene oxide (2.9 g, 50 mmol), an initial pressure of 3 MPa CO_2, substrate/catalyst = 5000, **Iq-POC** (12.1 mg, 0.01 mmol), $ZnBr_2$ (22.5 mg, 0.1 mmol), 120 °C. The selectivities of all the results were >99%. All the results were averaged over two runs, and (**b**) the recyclability test of catalyst **Iq-POC**. Reaction conditions: propylene oxide (5.8 g, 100 mmol), an initial pressure of 3 MPa CO_2, substrate/catalyst = 5000, **Iq-POC** (24.2 mg, 0.02 mmol), $ZnBr_2$ (45 mg, 0.2 mmol), 1 h, 120 °C.

Then, the recyclability test of the nucleophilic cage **Iq-POC** was performed in the model reaction of cycloadditon of CO_2 and propene oxide. Owing to the amplified cage structure, the nucleophilic cage **Iq-POC** is insoluble in propylene oxide and propylene carbonate; therefore, after the reaction, **Iq-POC** could be easily separated from the reaction system through filtration or centrifugation. To test the recyclability more accurately, a conversion of approximately 30% was chosen to evaluate whether there was a decline in activity, and the results show that recycling the **Iq-POC** cage over four runs did not lead to a significant loss of propylene carbonate yields (Figure 3b). Analysis of the reaction solution after each cycle by ICP (inductively coupled plasma) showed P and I element leaching did not reach the detection limit; however, we found $ZnBr_2$ salt is soluble in the reaction system; hence, the cocatalyst of $ZnBr_2$ salt has to be reloaded for the next run, while the **Iq-POC** was reused. Moreover, as shown in Figure 4, the versatility of our catalyst was further investigated. Under similar reaction conditions—though the reaction was prolonged for 10 h—satisfactory yields of corresponding cyclic carbonates were obtained, except for cyclohexene oxide (34% yield, 12 h), which was probably due to the steric hindrance of both the substrate and **Iq-POC**.
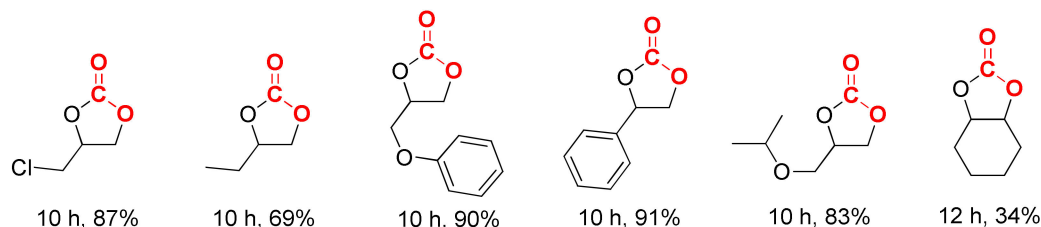

10 h, 87%   10 h, 69%   10 h, 90%   10 h, 91%   10 h, 83%   12 h, 34%

Figure 4. Reaction conditions: substrate (20 mmol), an initial pressure of 3 MPa CO_2, substrate/catalyst = 5000, **Iq-POC** (4.8 mg, 0.004 mmol), $ZnBr_2$ (9 mg, 0.04 mmol), 120 °C. The selectivities of all the results were >99%.

3. Materials and Experiments

3.1. General Remarks

Triphenylphosphine-based trialdehyde was synthesized according to [82,83]. All the other reagents were commercial grade and used without further purification. (R,R)-1,2-cyclohexanediamine (Alfa Aesar Co., Ltd., Tianjin, China), 4-bromobenzaldehyde diethyl

acetal (Energy Chemical Co., Ltd., Shanghai, China), phosphorus trichloride (Energy Chemical Co., Ltd.) and all the epoxides were purchased from J&K Scientific. Co., Ltd. (Shanghai, China) and Alfa Aesar Co., Ltd. The carbon dioxide used is commercially available with 99.99% purity.

Yields refer to isolated yields of compounds estimated to be ≥95% pure as determined by ^{1}H NMR (25 °C). The liquid NMR spectra were recorded on a Bruker AVANCE III NMR spectrometer (Bruker, Karlsruhe, Germany), 400 MHz for ^{1}H spectra and 100 MHz for ^{13}C spectra. Chemical shifts are reported as δ-values in ppm relative to the deuterated solvent peak: CDCl$_3$ (δ_H: 7.26; δ_C: 77.16). The high-resolution mass spectra (HRMS) data were collected on an Agilent Q-TOF6540 spectrometer (Agilent, Santa Clara, CA, USA). The single crystal X-ray diffraction data (SXRD) were collected on an Agilent GeminUltra diffractometer (Agilent, Santa Clara, CA, USA) with Mo Kα radiation, and liquid nitrogen purging was necessary to prevent crystal cracking. Inductively coupled plasma spectroscopy (ICP) was performed on a PerkinElmer apparatus Optima 7300 DV (PerkinElmer, Fremont, CA, USA). The N$_2$ adsorption experiment was performed on the Quantachrome Autosorb-1 instrument (Quantachrome, Boynton Beach, Florida, USA) at 77 K. GC analyses were performed on an Agilent 7890A (Agilent, Santa Clara, CA, USA) equipped with a capillary column (HP-5, 30 m length, 0.32 mm diameter), using a flame ionization detector.

3.2. Synthesis of the Cage **3**

Ethyl acetate (150 mL) was added to triphenylphosphine-based trialdehyde (1, 429 mg, 1.24 mmol) in a beaker at room temperature. The suspension was stirred with a glass rod and became clear. Next, a solution of (R,R)-1,2-cyclohexanediamine (2, 212 mg, 1.86 mmol) in ethyl acetate (30 mL) was added dropwise, and a turbid solution was observed during the addition process. The resulting mixture was left covered for 72 h without stirring. Some precipitation was formed after around 1–2 h. After reaction, the resulting mixture was filtrated, and the filtrate was concentrated to around 5 mL by using a rotary evaporator. Then 100 mL methanol was added to the precipitate the product as a white powder. The cage product (81% yield, 465 mg) was collected by filtration and dried under reduced pressure. ^{1}H NMR (CDCl$_3$, 400 MHz): δ (ppm) = 7.67 (s, 6H), 7.30 (d, 12H, J = 4.0 Hz), 6.99 (t, 12H, J = 8.0 Hz), 3.19 (t, 6H, J = 8.0 Hz), 2.13 (d, 6H, J = 12.0 Hz), 1.92 (d, 12H, J = 8.0 Hz), 1.51 (t, 6H, J = 12 Hz). ^{13}C NMR (CDCl$_3$, 100 MHz): δ (ppm) = 163.1, 139.1, 139.0, 136.6, 133.2, 133.0, 127.7, 127.6, 73.2, 32.0, 24.4. ^{31}P NMR (CDCl$_3$, 400 MHz): δ (ppm) = −7.8. Electrospray ionization high resolution mass spectrometry (ESI-HRMS): m/z calculation for [C$_{60}$N$_6$P$_2$H$_{60}$]: 926.4355; found 927.4415 [M + H]$^+$.

3.3. Synthesis of **Iq-POC**

Cage **3** (1.0 mmol, 0.93 g) was dissolved in 35 mL THF (tetrahydrofuran); then CH$_3$I (1.4 g, 10 mmol) was introduced to the cage solution. The mixed solution was refluxed for 48 h. After reaction, the cage **Iq-POC** was isolated by filtration and washed with THF (10 mL × 3). The crude product was dried under vacuum at 60 °C for 5 h to provide the final pure cage **Iq-POC** (1.1 g, 91% yield). Note: The cage **Iq-POC** was poorly soluble in almost all solvents, so it could not be characterized by liquid NMR. However, we obtained the HRMS spectrum; its molecular weight can be measured at very dilute concentrations. Electrospray ionization high resolution mass spectrometry (ESI-HRMS): m/z calculation for [C$_{62}$N$_6$P$_2$H$_{66}$]$^{2+}$: m/z = 478.7412, z = 2; found 478.2386. Solid-state ^{31}P NMR: δ (ppm) = 22.

3.4. General Procedure of Catalytic Reactions

Reactions were performed in a 25 mL autoclave with vigorous stirring. For a typical catalytic run, propylene oxide (1.16 g, 20 mmol), **Iq-POC** catalyst (4.8 mg, 0.004 mmol, substrate/catalyst = 5000) and ZnBr$_2$ (9 mg, 0.04 mmol) were added into the autoclave without any solvent. After sealing and purging with CO$_2$ 3 times, the pressure was adjusted to 3 MPa as an initial pressure. Then the autoclave was put into a preheated oil bath and the solution was stirred at 120 °C for several hours. After the reaction was completed, the

autoclave was cooled to ambient temperature, and the excess CO_2 was carefully vented. The catalyst was separated by filtration and the aqueous solutions containing the products were analyzed using gas chromatograph. n-Butanol was used as an internal standard and the GC was also calibrated using known amounts of substrate and products. The recycled catalyst could be reused for the next run.

4. Conclusions

In conclusion, in this work we have developed a novel ionic quasi-porous organic cage (**Iq-POC**) through dynamic covalent chemistry and a nucleophilic addition reaction. This quaternary phosphonium salt-type cage was applied as a nucleophilic catalyst for the cycloaddition reaction of CO_2 and epoxides. Satisfactory activity and substrate scope were achieved by using our catalytic system. Owing to the amplified cage structure, the nucleophilic cage **Iq-POC** is insoluble in propylene oxide and propylene carbonate; therefore, after reaction, **Iq-POC** could be easily separated from the reaction system through filtration. This "heterogenized cage catalyst" may be a new solution in the area of homogeneous catalyst recycling. However, it is a pity that the co-catalyst cannot be recycled at present; in pursuit of a complete catalyst cycle, we need to try other catalytic systems in the future. Other interesting cage catalysts are under development in our laboratory.

Supplementary Materials: The following are available online at https://www.mdpi.com/2073-4344/11/3/358/s1. Figure S1: ^{1}H NMR spectrum of cage **3**; Figure S2: ^{13}C NMR spectrum of cage **3**; Figure S3: ^{31}P NMR spectrum of cage **3**; Figure S4: Solid-state ^{31}P NMR spectrum of cage **Iq-POC**; Figure S5: Monoclinic space group C2 of cage **3**; Figure S6: The PXRD spectrum of **Iq-POC**; Figure S7: N_2 sorption isotherms of **Iq-POC** measured at 77 K; Figure S8: Proposed catalytic mechanism; Figure S9: ^{1}H NMR copies of known products.

References

1. Tozawa, T.; Jones, J.T.A.; Swamy, S.I.; Jiang, S.; Adams, D.J.; Shakespeare, S.; Clowes, R.; Bradshaw, D.; Hasell, T.; Chong, S.Y.; et al. Porous organic cages. *Nat. Mater.* **2009**, *8*, 973–978. [CrossRef] [PubMed]
2. Little, M.A.; Cooper, A.I. The chemistry of porous organic molecular materials. *Adv. Funct. Mater.* **2020**, *30*, 1909842. [CrossRef]
3. Mastalerz, M. Porous shape-persistent organic cage compounds of different size, geometry, and function. *Acc. Chem. Res.* **2018**, *51*, 2411–2422. [CrossRef]
4. Cooper, A.I. Porous molecular solids and liquids. *ACS Cent. Sci.* **2017**, *3*, 544–553. [CrossRef] [PubMed]
5. Briggs, M.E.; Cooper, A.I. A perspective on the synthesis, purification, and characterization of porous organic cages. *Chem. Mater.* **2017**, *29*, 149–157. [CrossRef] [PubMed]
6. Hasell, T.; Cooper, A.I. Porous organic cages: Soluble, modular and molecular pores. *Nat. Rev. Mater.* **2016**, *1*, 16053. [CrossRef]
7. Yu, N.; Ding, H.; Wang, C. Synthesis and application of organic molecular cages. *Prog. Chem.* **2016**, *28*, 1721–1731.
8. Slater, A.G.; Cooper, A.I. Function-led design of new porous materials. *Science* **2015**, *348*, aaa8075. [CrossRef]
9. Evans, J.D.; Sumby, C.J.; Doonan, C.J. Synthesis and applications of porous organic cages. *Chem. Lett.* **2015**, *44*, 582–588. [CrossRef]
10. Zhang, G.; Mastalerz, M. Organic cage compounds – from shape-persistency to function. *Chem. Soc. Rev.* **2014**, *43*, 1934–1947. [CrossRef]
11. Mastalerz, M. Shape-persistent organic cage compounds by dynamic covalent bond formation. *Angew. Chem. Int. Ed.* **2010**, *49*, 5042–5053. [CrossRef]

12. Acharyya, K.; Mukherjee, P.S. Organic imine cages: Molecular marriage and applications. *Angew. Chem. Int. Ed.* **2019**, *58*, 8640–8653. [CrossRef] [PubMed]

13. Jiao, T.; Wu, G.; Zhang, Y.; Shen, L.; Lei, Y.; Wang, G.-Y.; Fahrenbach, A.C.; Li, H. Self-assembly in water with N-substituted imines. *Angew. Chem. Int. Ed.* **2020**, *59*, 18350–18367. [CrossRef] [PubMed]

14. Belowich, M.E.; Stoddart, J.F. Dynamic imine chemistry. *Chem. Soc. Rev.* **2012**, *41*, 2003–2024. [CrossRef] [PubMed]

15. Liu, Y.; Li, Z.-T. A dynamic route for structure and function: Recent advances in imine-based organic nanostructured materials. *Aust. J. Chem.* **2013**, *66*, 9–22. [CrossRef]

16. Schneider, M.W.; Oppel, I.M.; Ott, H.; Lechner, L.G.; Hauswald, H.-J.S.; Stoll, R.; Mastalerz, M. Periphery-substituted [4+6] salicylbisimine cage compounds with exceptionally high surface areas: Influence of the molecular structure on nitrogen sorption properties. *Chem. Eur. J.* **2012**, *18*, 836–847. [CrossRef] [PubMed]

17. Zhu, Q.; Wang, X.; Clowes, R.; Cui, P.; Chen, L.; Little, M.A.; Cooper, A.I. 3D Cage COFs: A dynamic three-dimensional covalent organic framework with high-connectivity organic cage nodes. *J. Am. Chem. Soc.* **2020**, *142*, 16842–16848. [CrossRef]

18. Hasell, T.; Wu, X.; Jones, J.T.A.; Bacsa, J.; Steiner, A.; Mitra, T.; Trewin, A.; Adams, D.J.; Cooper, A.I. Triply interlocked covalent organic cages. *Nat. Chem.* **2010**, *2*, 750–755. [CrossRef]

19. Zhang, G.; Presly, O.; White, F.; Oppel, I.M.; Mastalerz, M. A permanent mesoporous organic cage with an exceptionally high surface area. *Angew. Chem. Int. Ed.* **2014**, *53*, 1516–1520. [CrossRef] [PubMed]

20. Elbert, S.M.; Regenauer, N.I.; Schindler, D.; Zhang, W.-S.; Rominger, F.; Schröder, R.R.; Mastalerz, M. Shape-persistent tetrahedral [4+6] boronic ester cages with different degrees of fluoride substitution. *Chem. Eur. J.* **2018**, *24*, 11438–11443. [CrossRef]

21. Brutschy, M.; Schneider, M.W.; Mastalerz, M.; Waldvogel, S.R. Porous organic cage compounds as highly potent affinity materials for sensing by quartz crystal microbalances. *Adv. Mater.* **2012**, *24*, 6049–6052. [CrossRef]

22. Brutschy, M.; Schneider, M.W.; Mastalerz, M.; Waldvogel, S.R. Direct gravimetric sensing of GBL by molecular recognition process in organic cage compounds. *Chem. Commun.* **2013**, *49*, 8398–8400. [CrossRef]

23. Hähsler, M.; Mastalerz, M. A giant [8+12] boronic ester cage with 48 terminal alkene units in the periphery for postsynthetic alkene metathesis. *Chem. Eur. J.* **2021**, *27*, 233–237. [CrossRef]

24. Takata, H.; Ono, K.; Iwasawa, N. Controlled release of the guest molecule via borate formation of fluorinated boronic ester cage. *Chem. Commun.* **2020**, *56*, 5613–5616. [CrossRef]

25. Li, H.-G.; Li, L.; Xu, H.; Wang, G.-W. Mechanochemical synthesis and properties of boronic ester cage compounds. *Curr. Org. Chem.* **2018**, *22*, 923–929. [CrossRef]

26. Takahagi, H.; Fujibe, S.; Iwasawa, N. Guest-induced dynamic self-assembly of two diastereomeric cage-like boronic esters. *Chem. Eur. J.* **2009**, *15*, 13327–13330. [CrossRef]

27. Tan, C.; Jiao, J.; Li, Z.; Liu, Y.; Han, X.; Cui, Y. Design and assembly of a chiral metallosalen-based octahedral coordination cage for supramolecular asymmetric catalysis. *Angew. Chem. Int. Ed.* **2018**, *57*, 2085–2090. [CrossRef]

28. Liu, M.; Zhang, L.; Little, M.A.; Kapil, V.; Ceriotte, M.; Yang, S.; Ding, L.; Holden, D.L.; Balderas-Xicohténcatl, R.; He, D.; et al. Barely porous organic cages for hydrogen isotope separation. *Science* **2019**, *366*, 613–620. [CrossRef]

29. Zhang, Q.; Li, H.; Chen, S.; Duan, J.; Jin, W. Mixed-matrix membranes with soluble porous organic molecular cage for highly efficient C_3H_6/C_3H_8 separation. *J. Memb. Sci.* **2020**, *611*, 118288. [CrossRef]

30. Lucero, J.M.; Carreon, M.A. Separation of light gases from xenon over porous organic cage membranes. *ACS Appl. Mater. Interfaces* **2020**, *12*, 32182–32188. [CrossRef]

31. Kunde, T.; Nieland, E.; Schroder, H.V.; Schalley, C.A.; Schmidt, B.M. A porous fluorinated organic [4+4] imine cage showing CO_2 and H_2 adsporption. *Chem. Commun.* **2020**, *56*, 4761–4764. [CrossRef] [PubMed]

32. Charles, C.D.; Bloch, E.D. High-pressure methane storage and selective gas adsorption in a cyclohexane-functionalised porous organic cage. *Supramol. Chem.* **2019**, *31*, 508–513. [CrossRef]

33. Jin, Y.; Voss, B.A.; Jin, A.; Long, H.; Noble, R.D.; Zhang, W. Highly CO_2-selective organic molecular cages: What determines the CO_2 selectivity. *J. Am. Chem. Soc.* **2011**, *133*, 6650–6658. [CrossRef]

34. Wang, Z.; Sikdar, N.; Wang, S.-Q.; Li, X.; Yu, M.; Bu, X.-H.; Chang, Z.; Zou, X.; Chen, Y.; Cheng, P.; et al. Soft porous crystal based upon organic cages that exhibit guest-induced breathing selective gas separation. *J. Am. Chem. Soc.* **2019**, *141*, 9408–9414. [CrossRef]

35. Yang, S.; Chen, L.; Holden, D.; Wang, R.; Cheng, Y.; Well, M.; Cooper, A.I.; Ding, L. Understanding the effect of host flexibility on the adsorption of CH_4, CO_2 and SF_6 in porous organic cages. *Kristallogr. Cryst. Mater.* **2019**, *234*, 547–555. [CrossRef]

36. Little, M.A.; Chong, S.Y.; Schmidtmann, M.; Hasell, T.; Copper, A. Guest control of structure in porous organic cages. *Chem. Commun.* **2014**, *50*, 9465–9468. [CrossRef] [PubMed]

37. Saini, M.; Verma, A.; Tomar, K.; Bharadwaj, P.K.; Sadhu, K.K. Regioisomeric cryptand stabilized gold supraspheres and elongated dodecahedron supraparticles for reversible host-guest chemistry. *Chem. Commun.* **2018**, *54*, 12836–12839. [CrossRef]

38. Lu, Z.; Lu, X.; Zhong, Y.; Hu, Y.; Li, G.; Zhang, R. Carbon dot-decorated porous organic cage as fluorescent sensor for rapid discrimination of nitrophenol isomers and chiral alcohols. *Anal. Chim. Acta* **2019**, *1050*, 146–153. [CrossRef] [PubMed]

39. Wang, B.-J.; Duan, A.-H.; Zhang, J.-H.; Xie, S.-M.; Cao, Q.-E.; Yuan, L.-M. An Enantioselective Potentiometric Sensor for 2-Amino-1-Butanol Based on Chiral Porous Organic Cage CC3-R. *Molecules* **2019**, *24*, 420. [CrossRef] [PubMed]

40. Duan, A.-H.; Wang, B.-J.; Xie, S.-M.; Zhang, J.-H.; Yuan, L.-M. A chiral, porous, organic cage-based, enantioselective potentiometric sensor for 2-aminobutanol. *Chirality* **2017**, *29*, 172–177. [CrossRef] [PubMed]

41. Li, H.-X.; Xie, T.-P.; Yan, K.-Q.; Xie, S.-M.; Wang, B.-J.; Zhang, J.-H.; Yuan, L.-M. A hydroxyl-functionalized homochiral porous organic cage for gas chromatography. *Microchim. Acta* **2020**, *187*, 269. [CrossRef]

42. Li, H.-X.; Xie, T.-P.; Xie, S.-M.; Wang, B.-J.; Zhang, J.-H.; Yuan, L.-M. Enantiomeric separation on a homochiral porous organic cage-based chiral stationary phase by gas chromatography. *Chromatographia* **2020**, *83*, 703–713. [CrossRef]

43. Zhang, J.-H.; Xie, S.-M.; Wang, B.-J.; He, P.-G.; Yuan, L.-M. A homochiral porous organic cage with large cavity and pore windows for the efficient gas chromatography separation of enantiomers and positional isomers. *J. Sep. Sci.* **2018**, *41*, 1385–1394. [CrossRef]

44. Zhang, J.-H.; Zhu, P.-J.; Xie, S.-M.; Zi, M.; Yuan, L.-M. Homochiral porous organic cage used as stationary phase for open tubular capillary electrochromatography. *Anal. Chim. Acta* **2018**, *999*, 169–175. [CrossRef] [PubMed]

45. McCaffrey, R.; Long, H.; Jin, Y.; Sanders, A.; Park, W.; Zhang, W. Template synthesis of gold nanoparticles with an organic molecular cage. *J. Am. Chem. Soc.* **2014**, *136*, 1782–1785. [CrossRef] [PubMed]

46. Nihei, M.; Ida, H.; Nibe, T.; Moeljadi, A.M.P.; Trinh, Q.T.; Hirao, H.; Ishizaki, M.; Kurihara, M.; Shiga, T.; Oshio, H. Ferrihydrite particle encapsulated within a molecular organic cage. *J. Am. Chem. Soc.* **2018**, *140*, 17753–17759. [CrossRef]

47. Yang, X.; Sun, J.-K.; Kitta, M.; Pang, H.; Xu, Q. Encapsulating highly catalytically active metal nanoclusters inside porous organic cages. *Nat. Catal.* **2018**, *1*, 214–220. [CrossRef]

48. Mondal, B.; Mukherjee, P.S. Cage Encapsulated Gold Nanoparticles as heterogeneous photocatalyst for facile and selective reduction of nitroarenes to azo compounds. *J. Am. Chem. Soc.* **2018**, *140*, 12592–12601. [CrossRef]

49. Mondal, B.; Acharyya, K.; Howlader, P.; Mukherjee, P.S. Molecular cage impregnated palladium nanoparticles: Efficient, additive-free heterogeneous catalysts for cyanation of aryl halides. *J. Am. Chem. Soc.* **2016**, *138*, 1709–1716. [CrossRef] [PubMed]

50. Qiu, L.; McCaffrey, R.; Jin, Y.; Gong, Y.; Hu, Y.; Sun, H.; Park, W.; Zhang, W. Cage-templated synthesis of highly stable palladium nanoparticles and their catalytic activities in Suzuki-Miyaura coupling. *Chem. Sci.* **2018**, *9*, 676–680. [CrossRef] [PubMed]

51. Sharma, V.; De, D.; Saha, R.; Chattaraj, P.K.; Bharadwaj, P.K. Flexibility induced encapsulation of ultrafine palladium nanoparticles into organic cages for Tsuji-Trost allylation. *ACS Appl. Mater. Interfaces* **2020**, *12*, 8539–8546. [CrossRef] [PubMed]

52. Verma, A.; Tomar, K.; Bharadwaj, P.K. Nanosized bispyrazole-based cryptand-stabilized palladium (0) nanoparticles: A resuable heterogeneous catalyst for the Suzuki-Miyaura coupling reaction in water. *Inorg. Chem.* **2019**, *58*, 1003–1006. [CrossRef]

53. Sharma, V.; Bharadwaj, P.K. Organic cage supported metal nanoparticles for applications. *Dalton Trans.* **2020**, *49*, 15574–15586. [CrossRef] [PubMed]

54. Sun, J.-K.; Zhan, W.-W.; Akita, T.; Xu, Q. Toward homogenization of heterogeneous metal nanoparticle catalysts with enhanced catalytic performance: Soluble porous organic cage as a stabilizer and homogenizer. *J. Am. Chem. Soc.* **2015**, *137*, 7063–7066. [CrossRef]

55. Zhang, Y.; Xiong, Y.; Ge, J.; Lin, R.; Chen, C.; Peng, Q.; Wang, D.; Li, Y. Porous organic cage stabilised palladium nanoparticles: Efficient heterogeneous catalysts for carbonylation reaction of aryl halides. *Chem. Commun.* **2018**, *54*, 2796–2799. [CrossRef]

56. Song, Q.; Wang, W.D.; Hu, X.; Dong, Z. Ru nanoclusters confined in porous organic cages for catalytic hydrolysis of ammonia borane and tandem hydrogenation reaction. *Nanoscale* **2019**, *11*, 21513–21521. [CrossRef] [PubMed]

57. Jiang, S.; Cox, H.J.; Papaioannou, E.I.; Tang, C.; Liu, H.; Murdoch, B.J.; Gibson, E.K.; Metcalfe, I.S.; Evan, J.S.O.; Beaumont, S.K. Shape-persistent porous organic cage supported palladium nanoparticles as heterogeneous catalytic materials. *Nanoscale* **2019**, *11*, 14929–14936. [CrossRef]

58. Chen, G.-J.; Xin, W.-L.; Wang, J.-S.; Cheng, J.-Y.; Dong, Y.-B. Visible-light triggered selective reduction of nitroarenes to azo compounds catalysed by Ag@organic molecular cages. *Chem. Commun.* **2019**, *55*, 3586–3589. [CrossRef] [PubMed]

59. Sun, N.; Wang, C.; Wang, H.; Yang, L.; Jin, P.; Zhang, W.; Jiang, J. Multifunctional tubular organic cage-supported ultrafine palladium nanoparticles for sequential catalysis. *Angew. Chem. Int. Ed.* **2019**, *58*, 18011–18016. [CrossRef]

60. Smith, P.T.; Benke, B.P.; Cao, Z.; Kim, Y.; Nichols, E.V.; Kim, K.; Chang, C.J. Iron porphyrin embedded into a supramolecular porous organic cage for electrochemical CO_2 reduction in water. *Angew. Chem. Int. Ed.* **2018**, *57*, 9684–9688. [CrossRef]

61. Liu, C.; Liu, K.; Wang, C.; Liu, H.; Wang, H.; Su, H.; Li, X.; Chen, B.; Jiang, J. Elucidating heterogeneous photocatalytic superiority of microporous porphyrin organic cage. *Nat. Commun.* **2020**, *11*, 1047. [CrossRef]

62. Koo, J.; Kim, I.; Kim, Y.; Cho, D.; Hwang, I.-C.; Mukhopadhyay, R.D.; Song, H.; Ko, Y.H.; Dhamija, A.; Lee, H.; et al. Gigantic porphyrinic cages. *Chem* **2020**, *6*, 3374–3384. [CrossRef]

63. Hussain, M.D.W.; Giri, A.; Patra, A. Organic nanocages: A promising testbed for catalytic CO_2 conversion. *Sustain. Energy Fuels* **2019**, *3*, 2567–2571. [CrossRef]

64. Shih, C.F.; Zhang, T.; Li, J.; Bai, C. Powering the future with liquid sunshine. *Joule* **2018**, *2*, 1–25. [CrossRef]

65. Aresta, M.; Dibenedetto, A.; Angelini, A. Catalysis for the valorization of exhaust carbon: From CO_2 to chemicals, materials, and fuels. Technological use of CO_2. *Chem. Rev.* **2014**, *114*, 1709–1742. [CrossRef] [PubMed]

66. Artz, J.; Mueller, T.; Thenert, K.; Kleinekorte, J.; Meys, R.; Sternberg, A.; Bardow, A.; Leitner, W. Sustainable conversion of carbon dioxide: An integrated review of catalysis and life cycle assessment. *Chem. Rev.* **2018**, *118*, 434–504. [CrossRef] [PubMed]

67. North, M.; Pasquale, R.; Young, C. Synthesis of cyclic carbonates from epoxides and CO_2. *Green Chem.* **2010**, *12*, 1514–1539. [CrossRef]

68. Martin, C.; Fiorani, G.; Kleij, A.W. Recent advances in the catalytic preparation of cyclic organic carbonates. *ACS Catal.* **2015**, *5*, 1353–1370. [CrossRef]

69. Shaikh, R.R.; Pornpraprom, S.; D'Elia, V. Catalytic strategies for the cycloaddition of pure, diluted, and waste CO_2 to epoxides under ambient conditions. *ACS Catal.* **2018**, *8*, 419–450. [CrossRef]

70. Huang, K.; Zhang, J.-Y.; Liu, F.; Dai, S. Synthesis of porous polymeric catalysts for the conversion of carbon dioxide. *ACS Catal.* **2018**, *8*, 9079–9102. [CrossRef]

71. Liu, H.; Huang, Z.; Han, Z.; Ding, K.; Liu, H.; Xia, C.; Chen, J. Efficient production of methanol and diols via the hydrogenation of cyclic carbonates using copper-silica nanocomposite catalysts. *Green Chem.* **2015**, *17*, 4281–4290. [CrossRef]

72. Han, Z.; Rong, L.; Wu, J.; Zhang, L.; Wang, Z.; Ding, K. Catalytic hydrogenation of cyclic carbonates: A practical approach from CO_2 and epoxides to methanol and diols. *Angew. Chem. Int. Ed.* **2012**, *51*, 13041–13045. [CrossRef] [PubMed]

73. Wang, W.; Li, C.; Yan, L.; Wang, Y.; Jiang, M.; Ding, Y. Ionic liquid/Zn-PPh$_3$ integrated porous organic polymers featuring multifunctional sites: Highly active heterogeneous catalyst for cooperative conversion of CO_2 to cyclic carbonates. *ACS Catal.* **2016**, *6*, 6091–6100. [CrossRef]

74. Li, F.; Xiao, L.; Xia, C.; Hu, B. Chemical fixation of CO_2 with highly efficient ZnCl$_2$/[BMIm]Br catalyst system. *Tetrahedron Lett.* **2004**, *45*, 8307–8310. [CrossRef]

75. Xu, B.-H.; Wang, J.-Q.; Sun, J.; Huang, Y.; Zhang, J.-P.; Zhang, X.-P.; Zhang, S.-J. Fixation of CO_2 into cyclic carbonates catalyzed by ionic liquids: A multi-scale approach. *Green Chem.* **2015**, *17*, 108–122. [CrossRef]

76. Cheng, W.; Su, Q.; Wang, J.; Sun, J.; Ng, F.T.T. Ionic liquids: The synergistic catalytic effect in the synthesis of cyclic carbonates. *Catalysts* **2013**, *3*, 878–901. [CrossRef]

77. Calo, V.; Nacci, A.; Monopoli, A.; Fanizzi, A. Cyclic carbonate formation from carbon dioxide and oxiranes in tetrabutylammonium halides as solvents and catalysts. *Org. Lett.* **2002**, *4*, 2561–2563. [CrossRef] [PubMed]

78. Tiffner, M.; Gonglach, S.; Haas, M.; Schofberger, W.; Waser, M. CO_2 Fixation with epoxides under mild conditions with a cooperative metal corrole/quaternary ammonium salt catalyst system. *Chem. Asian J.* **2017**, *12*, 1048–1051. [CrossRef]

79. Zhao, L.-Y.; Chen, J.-Y.; Li, W.-C.; Lu, A.-H. B$_2$O$_3$: A heterogeneous metal-free Lewis acid catalyst for carbon dioxide fixation into cyclic carbonates. *J. CO2 Util.* **2019**, *29*, 172–178. [CrossRef]

80. Sun, J.; Ren, J.; Zhang, S.; Cheng, W. Water as an efficient medium for the synthesis of cyclic carbonate. *Tetrahedron Lett.* **2009**, *450*, 423–426. [CrossRef]

81. Wang, W.; Cui, L.; Sun, P.; Shi, L.; Yue, C.; Li, F. Reusable N-heterocyclic carbene complex catalysts and beyond: A perspective on recycling strategies. *Chem. Rev.* **2018**, *118*, 9843–9929. [CrossRef] [PubMed]

82. Chalier, F.; Berchadsky, Y.; Finet, J.-P.; Gronchi, G.; Marque, S.; Tordo, P. Synthesis, X-ray geometry, and anodic behavior of tris[2-(hydroxymethyl)phenyl]phosphane. *J. Phys. Chem.* **1996**, *100*, 4323–4330. [CrossRef]

83. Bartlett, P.A.; Bauer, B.; Singer, S.J. Synthesis of water-soluble undecagold cluster compounds of potential importance in electron microscopic and other studies of biological systems. *J. Am. Chem. Soc.* **1978**, *100*, 5085–5089. [CrossRef]